The University of Wisconsin Library
Manuscript Theses

Unpublished theses submitted for the Master's and Doctor's degrees and deposited in The University of Wisconsin Library are open for inspection, but are to be used only with due regard to the rights of the authors. Bibliographical references may be noted, but passages may be copied only with the permission of the authors, and proper credit must be given in subsequent written or published work. Extensive copying or publication of the thesis in whole or in part requires also the consent of the Dean of the Graduate School of The University of Wisconsin.

This thesis by DAVID J. HART
has been used by the following persons, whose signatures attest their acceptance of the above restrictions.

A Library which borrows this thesis for use by its patrons is expected to secure the signature of each user:

NAME AND ADDRESS	DATE

Laboratory Measurements of a Complete Set of Poroelastic Moduli for Berea Sandstone and Indiana Limestone

by

David J. Hart

A thesis submitted in partial fulfillment of
the requirements for the degree of

Master of Science
(Geophysics)

at the

UNIVERSITY OF WISCONSIN-MADISON

1994

Acknowledgment

This research was supported by the Office of Basic Energy Science, Department of Energy, through grant DE-FG02-91ER14194 and was approved by Professor Herbert F. Wang.

I would like to thank my advisor, Herb Wang, for his guidance and support during this research. I would also like to thank my family for their support. Last I would like to thank my wife, Kris, for listening to all there was to hear about this research and doing the dishes even when it was my turn.

Table of Contents

Laboratory Measurements of a Complete Set of Poroelastic Moduli for Berea Sandstone and Indiana Limestone

Measurements have been completed for eight different poroelastic moduli of Berea Sandstone and Indiana Limestone as a function of confining pressure and pore pressure. The eight moduli measured were: drained bulk modulus, drained Young's modulus, drained Poisson's ratio, undrained bulk modulus, undrained Young's modulus, undrained Poisson's ratio, Skempton's coefficient, and the unjacketed solid frame modulus. The eight measurements constitute an overdetermined set for an isotropic material. The poroelastic moduli for Indiana Limestone are generally consistent to within 10%., which was verified by a formal inversion procedure for independent moduli from the eight measurements. The drained bulk modulus was 21.2 GPa, the undrained bulk modulus was 31.7 GPa, drained Poisson's ratio was 0.26, undrained Poisson's ratio was 0.33, and Skempton's coefficient was 0.47 at 30 MPa external stress. Internal inconsistencies occur for Berea Sandstone, possibly because the drained moduli are measured on dry samples. The dry shear modulus is significantly higher than the wet shear modulus, which is possibly due to chemical effects of water on the clay minerals.

Introduction

Elastic theory relates stress to strain. In linear elastic theory only two independent moduli are needed to characterize an elastic medium. If the medium is a fluid-filled porous material, then elastic theory may no longer completely describe the response of the medium to stresses. Nor will elastic theory predict the dilatation of the medium due to an increase in pore pressure. An extension of elastic theory to include the pore fluid is needed. Poroelastic theory provides this extension. Poroelastic theory relates strain to both stress and pore pressure. The constitutive equations describing this coupling require four poroelastic moduli (Biot, 1941; Rice and Cleary, 1976; Detournay and Cheng, 1993). It is the introduction of the pore fluid which makes necessary the two additional moduli.

Poroelastic theory can be applied to any elastic fluid-filled porous medium. It has been used to explain increased seismicity in an oil field (Segall, 1989); water table response to earth tides and barometric pressure (Van der Kamp and Gale, 1983); water table response to earthquakes (Bredehoeft, 1992; Carrigan, 1991); compaction of sedimentary basins (Bethke and Corbet, 1988) and hydraulic fracturing (Haimson and Fairhurst, 1969).

In this experiment eight poroelastic moduli were measured. The eight poroelastic moduli can be divided into three groups according to the pore fluid boundary condition applied during the test. The three conditions are drained, undrained and unjacketed.

The first group of moduli was found under drained conditions. In a drained condition there is no pore pressure response to external

stresses (Δp=0). This boundary condition is the same one usually assumed when finding elastic moduli. The moduli measured under drained conditions are the bulk modulus (K), Young's modulus (E), and Poisson's ratio (υ).

The second group of moduli was found under undrained conditions. Under undrained conditions there is no change in the volumetric pore fluid mass (Δm_f=0). The volumetric pore fluid mass, Δm_f, is the change in fluid mass per unit volume of the medium. The volumetric change in the water volume, $v_f - v_{fo}$, is the change in pore fluid volume per unit volume of the medium. The volumetric pore fluid mass change is related to the volumetric change in the water volume by using the density of the pore fluid, $\Delta m_f = \rho_o (v_f - v_{fo})$ where ρ_o is the pore fluid density. Under undrained conditions there can be a change in the pore pressure due to the external stress. The moduli measured under undrained conditions are the undrained bulk modulus (K_u), the undrained Young's modulus (E_u), the undrained Poisson's ratio(υ_u) and Skempton's coefficient (B).

The last modulus is measured under unjacketed conditions. Here the pore pressure change is made exactly equal to the external stress change (Δp=ΔPc). The modulus measured is the bulk grain modulus, also called the unjacketed solid frame modulus, (K_s).

Since only four moduli will uniquely describe a poroelastic medium, the eight measured moduli form an overdetermined set. A nonlinear inversion routine was used to calculate a best fit set of four poroelastic moduli. This set of moduli was then used to calculate best fit values for the other four moduli. The inversion minimized a root

mean squared residual between the observed moduli and the best fit moduli.

It is hoped measurements of complete sets of the poroelastic moduli will result in better models of poroelastic phenomena. A comparison of the best fit values to the measured values will also enable the experimenter to test the applicability of poroelastic theory to the medium being tested.

Poroelastic Theory

The development of the constitutive equations for poroelasticity given here follow the same arguments given in Biot (1941) and Rice and Cleary (1976). Special emphasis is given to finding relationships between poroelastic and elastic moduli. This is done because the inversion of the measured moduli to a best fit set of moduli uses relationships between the moduli.

The method for finding relationships between elastic moduli is first shown. Then development of the constitutive equations for poroelasticity will be done.

The constitutive equation for linear elasticity can be written

$$2G\varepsilon_{ij} = \sigma_{ij} - \frac{1}{3}\left(1 - \frac{2G}{3K}\right)\sigma_{kk}\delta_{ij}.$$

Here the shear modulus (G) and the bulk modulus (K) are moduli which relate the stress, σ_{ij}, to the strain, ε_{ij}. δ_{ij} is the Kronecker delta, which is zero when $i \neq j$ and one when $i = j$.

Relationships between three elastic moduli can be found using the constitutive equation and the definition of the third modulus. In this example Young's modulus will be related to the bulk modulus and the

shear modulus. Young's modulus is defined as

$$E = \left.\frac{\sigma_{11}}{\varepsilon_{11}}\right|_{\sigma_{22}=\sigma_{33}=0}.$$

If the boundary conditions for Young's Modulus, $\sigma_{22} = \sigma_{33} = 0$, are applied to the constitutive equation the resulting equation is

$$2G\varepsilon_{11} = \sigma_{11} - \frac{1}{3}\left(1 - \frac{2G}{3K}\right)\sigma_{11}.$$

This equation can be rearranged so that

$$\frac{\sigma_{11}}{\varepsilon_{11}} = \frac{9KG}{3K+G}.$$

Since $E = \frac{\sigma_{11}}{\varepsilon_{11}}$, then Young's modulus is related to the shear modulus and the bulk modulus by

$$E = \frac{9KG}{3K+G}.$$

Relationships between any three elastic moduli can be found in this manner.

When the elastic medium is porous and fluid-filled another term to include the effect of pore pressure on the strain of the medium is added to the elastic constitutive equation. The equation is written

$$\varepsilon_{ij} = \frac{\sigma_{ij}}{2G} - \frac{1}{3}\left(\frac{1}{2G} - \frac{1}{3K}\right)\sigma_{kk}\delta_{ij} + \frac{1}{H'}p\delta_{ij}.$$

ε_{ij} is the strain, σ_{ij} is the stress, and p is the pore pressure. G and K are the shear modulus and bulk modulus as in the elastic equation above. The plus sign in front of the pressure term denotes compressive stress and strain as positive. A third modulus, H', scales the strain due to the pore pressure. This is the first constitutive equation for poroelasticity. Another constitutive equation is needed to relate the increment of water volume per unit volume of the medium. This equation is written

$$v_f - v_{f0} = \frac{1}{3H}\sigma_{kk} + \frac{p}{R}.$$

$v_f - v_{f0}$ is the increment of water volume change per unit volume of the medium. H is a modulus relating stress to the water volume change and R is another modulus relating pore pressure to the water volume change. This is the second equation of poroelasticity. It appears that there are five poroelastic moduli (G,K,H',H,R) needed to relate stress, pore pressure, strain and water volume change.

It will be shown that $H' = H$ so that only four poroelastic moduli are needed to form a complete set of poroelastic moduli. An assumption of reversibility is made. In other words, the work done on the system is independent of the path taken to do that work. This can be written in terms of the work increment as

$$dW = \sigma_{ij}d\varepsilon_{ij} + pd(v_f - v_{f0}) = \varepsilon_{ij}d\sigma_{ij} + (v_f - v_{f0})dp.$$

This implies

$$\frac{\partial \varepsilon_{ij}}{\partial p} = \frac{\partial (v_f - v_{f0})}{\partial \sigma_{ij}}.$$

When the differentiation is carried out on the two constitutive equations for poroelasticity it is seen that

$$\frac{1}{3H} = \frac{1}{3H'}.$$

So only four moduli are needed to characterize a porous fluid filled elastic medium.

Other choices for the set of four poroelastic moduli can be made following a method similar to the one used to rewrite the elastic equations. Rice and Cleary (1976) recast the poroelastic constitutive equations, replacing the moduli K, H and R with Poisson's ratio (υ),

undrained Poisson's ratio (υ_u) and Skempton's coefficient (B). The definitions of these moduli are

$$\upsilon = -\left.\frac{\varepsilon_{22}}{\varepsilon_{11}}\right|_{dP_f=0,\sigma_{22}=\sigma_{33}=0}, \quad \upsilon_U = -\left.\frac{\varepsilon_{22}}{\varepsilon_{11}}\right|_{dm_f=0,\sigma_{22}=\sigma_{33}=0} \text{ and } B = \left.\frac{\partial p}{\partial P_c}\right|_{dm_f=0}.$$

The same steps used to rewrite the constitutive elastic equation with different moduli can be used to rewrite the constitutive equations for poroelasticity. Those steps are as follows. First the constitutive equations and the definition, including boundary conditions, of the modulus to be substituted are used to find a relationship between the four moduli currently in the constitutive equations and the fifth modulus. The relationship between the moduli is used to substitute the new modulus into the constitutive equations, removing one of the previously used moduli.

First Poisson's ratio will be substituted for the bulk modulus. The relationship between the bulk modulus (K), the shear modulus (G) and Poisson's ratio (υ) is

$$K = \frac{2G(1+\upsilon)}{3(1-2\upsilon)}.$$

When this is substituted for K in the constitutive equations, the result is

$$2G\varepsilon_{ij} = \sigma_{ij} - \frac{\upsilon}{(1+\upsilon)}\sigma_{kk}\delta_{ij} + \frac{2G}{3H}p\delta_{ij} \quad \text{and} \quad v_f - v_{f0} = \frac{1}{3H}\sigma_{kk} + \frac{p}{R}.$$

Next R is replaced by B. The definition of B and constitutive equation relating the volume change of water to stress and pressure give the relationship,

$$R = HB.$$

The constitutive equations are now written as

$$2G\varepsilon_{ij} = \sigma_{ij} - \frac{\upsilon}{(1+\upsilon)}\sigma_{kk}\delta_{ij} + \frac{2G}{3H}p\delta_{ij} \quad \text{and} \quad v_f - v_{f0} = \frac{1}{3H}\sigma_{kk} + \frac{p}{HB}.$$

Last, the undrained Poisson's ratio will be used to replace H. Again using the definition and boundary conditions of undrained Poisson's ratio a relationship between the moduli is found. That relationship is

$$\frac{2G}{H}=\frac{3(\upsilon_u-\upsilon)}{(\upsilon_u+1)(\upsilon+1)B}.$$

When this relationship is substituted for H the constitutive equations become

$$2G\varepsilon_{ij}=\sigma_{ij}-\frac{\upsilon}{(1+\upsilon)}\sigma_{kk}\delta_{ij}+\frac{3(\upsilon_u-\upsilon)}{B(1+\upsilon_u)(1+\upsilon)}p\delta_{ij} \text{ and } v_f-v_{f0}=\frac{3(\upsilon_u-\upsilon)}{B(1+\upsilon_u)(1+\upsilon)}[\sigma_{kk}+\frac{3}{B}p]$$

These equations are of the same form as those in Rice and Cleary (1976) except the volumetric change in pore fluid is replaced there by a change in the pore fluid mass by using the density, ρ_o.

Again the method for finding the relationships between poroelastic moduli is to first define the modulus and its boundary conditions and use the definition with the constitutive equations to arrive at the relationship between moduli. This method for finding the relationships between moduli was used later in this text to give relationships between the eight measured moduli. Those relationships were used in the inversion to find the best fit set of moduli.

Sample description

Berea Sandstone and Indiana Limestone were used as the rock samples. These two rocks were chosen because they had been previously used to measure a poroelastic modulus other than a drained elastic modulus. Also properties such as porosity, grain size and type

and percentage of mineral constituents are known for Berea Sandstone and Indiana Limestone.

Measurements and references for measurements of elastic moduli for Berea Sandstone can be found in the Handbook on the Mechanical Properties of Rocks (1978). Measurements of Skempton's coefficient (B) have been made by Berge, Wang and Bonner (1993) and Green and Wang (1986). Measurements of the unjacketed bulk modulus (Ks) and three elastic moduli, Poisson's ratio (υ), Young's modulus (E) and the bulk modulus (K), were made by Huang (1989) for Indiana Limestone.

Berea Sandstone is a medium-grained Mississippian greywacke. It is composed of quartz (~80 percent), feldspar(~5 percent), clay, predominantly kaolinite (~8 percent), and calcite (~6 percent). Its grains are well sorted (~155 μ) and subangular with quartz overgrowths. It has a porosity of 19%.

Indiana Limestone is of Mississippian age. It is composed of calcium carbonate (~98.21 percent), magnesium carbonate (~.075 percent), ferric oxide (~0.21 percent). The rest of the constituents (~0.83 percent) are insoluble. Some grains are actual oölites while others are merely coated with calcium carbonate. The grains are cemented by calcium carbonate. It has a porosity of 13%.

Modulus definitions

Measurements of poroelastic moduli were made by controlling the pore fluid boundary conditions and the external stress applied to a sample. The definition of the modulus of interest was used to set the stress and pore fluid boundary conditions. The resulting strains and

pore pressure changes were then recorded. The poroelastic moduli and their boundary conditions are shown below.

Drained

Bulk Modulus

$$K = -V\left.\frac{\partial P_c}{\partial V}\right|_{dP_f=0}$$

Young's Modulus

$$E = \left.\frac{\sigma_{11}}{\varepsilon_{11}}\right|_{dP_f=0,\sigma_{22}=\sigma_{33}=0}$$

Poisson's Ratio

$$\nu = -\left.\frac{\varepsilon_{22}}{\varepsilon_{11}}\right|_{dP_f=0,\sigma_{22}=\sigma_{33}=0}$$

Undrained

Bulk Modulus

$$K_U = -V\left.\frac{\partial P_c}{\partial V}\right|_{dm_f=0}$$

Young's Modulus

$$E_U = \left.\frac{\sigma_{11}}{\varepsilon_{11}}\right|_{dm_f=0,\sigma_{22}=\sigma_{33}=0}$$

Poisson's Ratio

$$\nu_U = -\left.\frac{\varepsilon_{22}}{\varepsilon_{11}}\right|_{dm_f=0,\sigma_{22}=\sigma_{33}=0}$$

Skempton's Coefficient

$$B = \left.\frac{\partial p}{\partial P_c}\right|_{dm_f=0}$$

Unjacketed

Bulk Grain Modulus

$$K_S = -V\left.\frac{\partial P_C}{\partial V}\right|_{dP_f=dP_C}$$

As can be seen from the definitions of the moduli, the slopes of various stress versus strain or pore pressure curves will give the poroelastic modulus of interest. For example Young's modulus is the slope of an axial stress versus an axial strain curve.

Experimental procedure

A total of four Berea Sandstone samples, T4, T7, T8 and T9, and two Indiana Limestone samples, InL1 and InL2, were tested. Sample T4 was cored with its axis parallel to the bedding plane. The other Berea Sandstone samples were cored with their axes perpendicular to the bedding plane. The Indiana Limestone samples were cored with their axes perpendicular to the bedding plane.

The samples were typically 5 cm in diameter and 8 cm in length. Micro-Measurements Strain gages model EA-060500BH-120 were chosen to measure the strains. The gages had dimensions of 1.27 cm length by 0.64 cm width. They were applied using Micro-Measurements M-Bond AE-10 Epoxy. A BLH 1200B strain gage indicator and a BLH 1225 switching and balancing unit were used to produce output. Two strain gages were aligned 180° apart and glued parallel to the sample axis. These two strain gages measured the axial strain. Two additional strain gages were aligned 180° apart and glued perpendicular to the sample axis. These two strain gages measured the circumferential strain. Solder tabs and lead wires were applied to prevent strain caused by possible tension on the lead wires.

RTV Silicone gel was then applied to the entire side of the sample, not the ends, and two tygon sleeves were fitted and clamped over the ends of the sample. This arrangement prevented leakage around the strain gage leads and enabled us to remove the endcaps after a drained run and saturate the sample for an undrained run.

A solid steel endcap was slid into the top tygon sleeve and clamped into place. The lower endcap contained a Kulite HKM-375 20 kpsi pressure transducer. A Sensotec Model GM signal conditioner/indicator was connected to produce the output. The transducer is slightly recessed into the endcap to prevent damage from contact with the sample. This transducer measured the pore pressure without significantly increasing the pore space of a sample (Green and Wang, 1986). This endcap was slid into the lower sleeve and clamped. Figure 1 shows the sample assembly.

The sample was then placed in a triaxial vessel. It was run through a seasoning cycle before any measurements were made. The seasoning cycle consisted of raising the confining stress from 0 Pa to 35 MPa over five minutes time. The sample was then put through a cycle of 0 to 35 MPa confining stress three more times with each cycle lasting about one minute.

At this point the sample was ready to be tested under drained conditions. Even though air was present as a pore fluid, air is so compressible that there was no pore fluid response to external stress. This gives a drained condition (Δp=0). The external confining pressure, P_c, was measured using a BLH DHF 10 kpsi pressure transducer and a Daytronic 3000-series conditioner/indicator. The axial load was measured using a BLH C2P1 2000lbs load cell and a BLH Model LCi load cell instrument. The triaxial vessel was used to apply the appropriate stress boundary conditions and the strains were recorded. Samples T4, T7, T8, InL1, and InL2 were tested dry. Sample T9 was tested wet using a hollow endcap with an air filled volume to give drained conditions with a wet sample. This was done to see if there was any difference between a drained wet sample or a drained dry sample.

To measure the drained bulk modulus (K), the confining pressure, a hydrostatic stress ($\sigma_{11} = \sigma_{22} = \sigma_{33}$), was brought to 27.6 MPa. The circumferential and axial strains were recorded. The confining pressure was raised in increments of 0.69 MPa and measurements of the strain were recorded. When the confining stress reached 41.4 MPa the test was ended.

The Young's modulus and Poisson's ratio were measured next. The confining pressure was lowered to 27.6 MPa. The hydraulic ram brought a piston in contact with the top endcap of the sample assembly. The axial stress, σ_{11}, was raised to 30.7 MPa. The circumferential strain ($\varepsilon_{\theta\theta}$) and axial strain ($\varepsilon_{zz}$) were measured. The axial stress (σ_{zz}) was incremented by 0.9 MPa while the confining pressure (σ_{rr}) was held constant at 27.6 MPa. When the axial stress reached 43.9 MPa, the test was ended.

When measurements necessary for calculation of the drained moduli were completed, the sample was removed from the vessel and the endcaps were removed. The sample was then evacuated under vacuum for at least one hour. It was immersed in deionized water for at least 30 minutes. The end caps were replaced and clamped. The sample was replaced in the triaxial vessel and was ready for testing under undrained conditions. The stresses were applied and the strains recorded the same as for the drained moduli.

In the case of samples T8, T9, InL1 and InL2 the samples were over saturated when attempting the first undrained test. That is they had a B=1, Δp=ΔPc, and so were under an unjacketed pore pressure boundary condition. These tests gave the unjacketed bulk modulus (Ks) for the above samples. These samples were then removed from the vessel and excess water was removed. They were then tested under undrained conditions.

In the cases of samples T4 and T7, after completing the undrained measurements the sample was removed and allowed to dry. The sample jacket was punctured. The sample was evacuated and then saturated

with hydraulic oil. The sample was once again placed in the triaxial vessel and measurements of the unjacketed bulk modulus were made. The stresses for this modulus were applied in the same manner as for the drained bulk modulus.

Experimental Results

Graphs for Berea Sandstone Sample T4 and Indiana Limestone Sample InL1 are attached as Figures 2 and 3. The slopes of the graphs give the modulus of interest. Note that

$$\varepsilon_{11} = -\frac{\Delta l}{l} \text{ and } \varepsilon_t = \frac{1}{3}(\varepsilon_{11} + \varepsilon_{22} + \varepsilon_{33}) = -\frac{\Delta V}{V}.$$

This removes a discrepancy between the sign of the slope of the plotted data and the moduli. Below are the results for all the recorded samples.

Table 1: Measured Poroelastic Moduli at 30 MPa Mean Stress

Sample	K (GPa)	E (GPa)	υ	Ku(GPa)	Eu (GPa)	υu	B	Ks(GPa)
Berea Sandstone Sample T4[1]	13.4	27.7	.152	16.8	18.6	.369	.715	35.4
Berea Sandstone Sample T7	13.1	23.6	.132	15.0	16.9	.305	.843	26.5
Berea Sandstone Sample T8	13.7	23.5	.124	12.3	13.3	.374	.860	26.1
Berea Sandstone Sample T9[2]	14.1	26.1	.166	15.6	13.5	.293	.868	30.8
Average of Berea Sandstone Samples	13.6	25.2	.144	14.9	15.6	.335	.822	29.7
Indiana Limestone Sample InL1	22.0	32.2	.245	30.6	27.5	.395	.504	71.0
Indiana Limestone Sample InL2	22.9	29.7	.250	30.7	38.0	.319	.432	74.4

1. Axis is parallel to bedding. All other samples have their axes perpendicular to bedding
2. The drained values were measured wet.

The error in a measurement is around ten percent. This is the sum of given instrument error and the difference in slopes at ±5 MPa.

Introduction to Inversion

Only four of the above moduli for a sample would be needed to characterize that sample according to poroelasticity. However if this is attempted one finds that the calculated value of an independent modulus doesn't have the same value as the modulus found by experimental means. As an example Skempton's coefficient (B) is calculated using the relationship

$$B = \frac{(1 - \frac{K}{K_u})}{(1 - \frac{K}{K_s})}$$

and values for K, Ku and Ks from Berea Sandstone Sample T4. The relationship was found by using the definitions of the moduli and substituting those definitions into the constitutive equations. The derivation of the relationship is carried out in Appendix A.

The calculated Skempton's Coefficient is B=0.32. This value is less than half of the value found experimentally, B=0.72. An inversion using all eight experimental moduli and poroelastic relationships between those moduli would minimize the overall differences or residuals between calculated values of the moduli and experimentally found values of the moduli.

The concept is the same one used to find a best fit line. Only two points are needed to define a line. However those two points may not accurately predict the slope and y-intercept and will give no indication of the linearity of the phenomenon. If three or more points are measured and a best fit line is found, then the linearity of the

phenomenon can be judged. If the phenomenon is linear, then that best fit line would most likely represent the physical phenomenon being studied .

Thus inversion of the poroelastic moduli has two purposes. The first is a test of how well poroelasticity can represent the medium, assuming there is no systematic error due to experimental technique. If there is a consistent bias in the moduli, then it would be very difficult to separate error in technique from a divergence from theory. If a medium appears to behave according to poroelastic theory, then the inversion can fulfill its second purpose which is to give a set of parameters which will better represent the medium according to poroelastic theory.

General Nonlinear Inversion

The relationships between the moduli are generally nonlinear so a nonlinear inversion scheme is used. A nonlinear inversion must have a set of data, $\bar{\mathbf{b}}$, a set of parameters, $\bar{\mathbf{x}}$, and a model relating the data to the parameters, $\mathbf{M}(\bar{\mathbf{x}}) = \bar{\mathbf{b}}$. $\bar{\mathbf{b}}$ and $\bar{\mathbf{x}}$ can be thought of as vectors. It is unlikely a model operating on any set of parameters will exactly fit a set of experimental data. This was seen when the calculated value of Skempton's coefficient (B) was less than half of the measured value. The purpose of the inversion is to find a set of parameters which will minimize the differences between the model calculated values and the experimentally found values. The difference between the model values and the experimental values is called the residual,

$$\mathbf{M}(\bar{\mathbf{x}}) - \bar{\mathbf{b}} = \bar{\mathbf{r}}.$$

A Taylor series expansion of the model is used to locally linearize the inversion,

$$\mathbf{M}(\bar{\mathbf{x}}+\overline{\Delta\mathbf{x}}) = \mathbf{M}(\bar{\mathbf{x}}) + \bar{\nabla}\mathbf{M}(\bar{\mathbf{x}})\overline{\Delta\mathbf{x}} + \cdots .$$

$\overline{\Delta\mathbf{x}}$ is a change in the parameters and $\bar{\nabla}\mathbf{M}(\bar{\mathbf{x}})$, a matrix of partial derivatives, is the Jacobian of the model, $\mathbf{M}(\bar{\mathbf{x}})$. The higher order terms of the Taylor series are dropped and the series is rearranged so that

$$\mathbf{M}(\bar{\mathbf{x}}) - \mathbf{M}(\bar{\mathbf{x}}+\overline{\Delta\mathbf{x}}) \approx \bar{\nabla}\mathbf{M}(\bar{\mathbf{x}})\overline{\Delta\mathbf{x}}.$$

It can now be seen that if

$$-\bar{\nabla}\mathbf{M}(\bar{\mathbf{x}})\overline{\Delta\mathbf{x}} = \bar{\mathbf{r}}$$

then

$$\mathbf{M}(\bar{\mathbf{x}}+\Delta\bar{\mathbf{x}}) \approx \bar{\mathbf{b}}.$$

Thus the model will better approximate the data when it uses the parameter set, $\bar{\mathbf{x}}+\Delta\bar{\mathbf{x}}$.

The problem remains to find the change in parameters, $\Delta\bar{\mathbf{x}}$. By taking the Taylor Series and dropping the higher order terms the model was locally linearized. The linear least squares inversion described in Menke (1989) can now be used to find $\Delta\bar{\mathbf{x}}$. Values for the Jacobian and the residual are calculated. They are then used in the least squares inversion to calculate the change in parameters.

To simplify the notation let

$$\bar{\mathbf{A}} = -\bar{\nabla}\mathbf{M}(\bar{\mathbf{x}}).$$

Now $\overline{\mathbf{A}\Delta\mathbf{x}} = \bar{\mathbf{r}}$ gives $\overline{\Delta\mathbf{x}} = (\overline{\mathbf{A}\,\mathbf{A}^{t}})\overline{\mathbf{A}^{t}\mathbf{r}}$, by the least squares inversion.

A new set of parameters is found by adding the change in parameters to the current set of parameters.

$$\overline{\mathbf{x}_{new}} = \overline{\mathbf{x}_{current}} + \overline{\Delta\mathbf{x}}$$

A new residual and Jacobian are then calculated using the new parameters. The process of calculating a change in parameters is repeated until the change in the residual between iterations becomes very small, i.e. there is closure.

Poroelastic Moduli Inversion

The eight measured moduli are taken as the data vector ($\bar{\mathbf{b}}$) and K_p, E_p, Ku_p, and Ks_p are taken as the independent parameter vector ($\bar{\mathbf{x}}$).

$$\bar{\mathbf{b}} = \begin{bmatrix} \mathbf{K}_e \\ \mathbf{E}_e \\ \mathbf{Ku}_e \\ \mathbf{Ks}_e \\ \upsilon_e \\ \mathbf{B}_e \\ \upsilon_{ue} \\ \mathbf{Eu}_e \end{bmatrix} \qquad \bar{\mathbf{x}} = \begin{bmatrix} \mathbf{K}_p \\ \mathbf{E}_p \\ \mathbf{Ku}_p \\ \mathbf{Ks}_p \end{bmatrix}$$

The model which acts on the parameters, $\bar{\mathbf{x}}$, is

$$\mathbf{M}(\bar{\mathbf{x}}) = \begin{bmatrix} \mathbf{K}_p \\ \mathbf{E}_p \\ \mathbf{Ku}_p \\ \mathbf{Ks}_p \\ \upsilon(\mathbf{K}_p, \mathbf{E}_p) \\ \mathbf{B}(\mathbf{K}_p, \mathbf{Ku}_p, \mathbf{Ks}_p) \\ \upsilon_u(\mathbf{K}_p, \mathbf{E}_p, \mathbf{Ku}_p, \mathbf{Ks}_p) \\ \mathbf{E}_u(\mathbf{K}_p, \mathbf{E}_p, \mathbf{Ku}_p, \mathbf{Ks}_p) \end{bmatrix}$$

where

$$\upsilon(\mathbf{K}_p,\mathbf{E}_p)=\frac{1}{2}-\frac{\mathbf{E}_p}{6\mathbf{K}_p}\quad,$$

$$\mathbf{B}(\mathbf{K}_p,\mathbf{Ku}_p,\mathbf{Ks}_p)=\frac{1-\dfrac{\mathbf{K}_p}{\mathbf{Ku}_p}}{1-\dfrac{\mathbf{K}_p}{\mathbf{Ks}_p}},$$

$$\upsilon_{\mathbf{u}}(\mathbf{K}_p,\mathbf{Ku}_p,\mathbf{Ks}_p)=\frac{3\upsilon+\mathbf{B}(1-2\upsilon)(1-{}^{\mathbf{K}_p}\!/_{\mathbf{Ks}_p})}{3-\mathbf{B}(1-2\upsilon)(1-{}^{\mathbf{K}_p}\!/_{\mathbf{Ks}_p})}\quad,$$

and $$\mathbf{E}_{\mathbf{u}}(\mathbf{K}_p,\mathbf{Ku}_p,\mathbf{Ks}_p)=3\mathbf{Ku}_p(1-2\upsilon_{\mathbf{u}}).$$

Note that υ and $\mathbf{B}$ when used to calculate the model value for $\upsilon_{\mathbf{u}}$ are calculated from the parameter set and are not experimental values. The same applies to the model value of $\mathbf{E}_{\mathbf{u}}$. The value of $\upsilon_{\mathbf{u}}$ used to calculate $\mathbf{E}_{\mathbf{u}}$ was calculated from the model parameter values and is not the experimentally found $\upsilon_{\mathbf{u}}$. The relationships between the moduli are derived in Appendix A.

The Jacobian and the residual are normalized so that no modulus is weighted more than another. This makes the assumption that all the measurements for the moduli are equally reliable and the proportion of error in a modulus to the value for the measured modulus is the same for all the moduli.

The normalized residual is

$$\bar{\mathbf{r}} = \begin{bmatrix} \frac{K_e - K_p}{K_e} \\ \frac{E_e - E_p}{E_e} \\ \frac{Ku_e - Ku_p}{Ku_e} \\ \frac{Ks_e - Ks_p}{Ks_e} \\ \frac{\upsilon_e - \upsilon(K_p, E_p)}{\upsilon_e} \\ \frac{B_e - B(K_p, Ku_p, Ks_p)}{B_e} \\ \frac{\upsilon_{u_e} - \upsilon_u(K_p, E_p, Ku_p, Ks_p)}{\upsilon_{u_e}} \\ \frac{Eu_e - Eu(K_p, E_p, Ku_p, Ks_p)}{Eu_e} \end{bmatrix} = \begin{bmatrix} 1 - \frac{K_p}{K_e} \\ 1 - \frac{E_p}{E_e} \\ 1 - \frac{Ku_p}{Ku_e} \\ 1 - \frac{Ks_p}{Ks_e} \\ 1 - \frac{\upsilon(K_p, E_p)}{\upsilon_e} \\ 1 - \frac{B(K_p, Ku_p, Ks_p)}{B_e} \\ 1 - \frac{\upsilon_u(K_p, E_p, Ku_p, Ks_p)}{\upsilon_{u_e}} \\ 1 - \frac{Eu(K_p, E_p, Ku_p, Ks_p)}{Eu_e} \end{bmatrix}$$

Here the normalized Jacobian is a 8 x 4 matrix.

$$\nabla \mathbf{M}(\bar{\mathbf{x}}) = \begin{bmatrix} \frac{\partial K_p}{\partial K_p}\frac{1}{K_e} & \frac{\partial K_p}{\partial E_p}\frac{1}{K_e} & \frac{\partial K_p}{\partial Ku_p}\frac{1}{K_e} & \frac{\partial K_p}{\partial Ks_p}\frac{1}{K_e} \\ \frac{\partial E_p}{\partial K_p}\frac{1}{E_e} & \frac{\partial E_p}{\partial E_p}\frac{1}{E_e} & \frac{\partial E_p}{\partial Ku_p}\frac{1}{E_e} & \frac{\partial E_p}{\partial Ks_p}\frac{1}{E_e} \\ \frac{\partial Ku_p}{\partial K_p}\frac{1}{Ku_e} & \frac{\partial Ku_p}{\partial E_p}\frac{1}{Ku_e} & \frac{\partial Ku_p}{\partial Ku_p}\frac{1}{Ku_e} & \frac{\partial Ku_p}{\partial Ks_p}\frac{1}{Ku_e} \\ \frac{\partial Ks_p}{\partial K_p}\frac{1}{Ks_e} & \frac{\partial Ks_p}{\partial E_p}\frac{1}{Ks_e} & \frac{\partial Ks_p}{\partial Ku_p}\frac{1}{Ks_e} & \frac{\partial Ks_p}{\partial Ks_p}\frac{1}{Ks_e} \\ \frac{\partial \upsilon}{\partial K_p}\frac{1}{\upsilon_e} & \frac{\partial \upsilon}{\partial E_p}\frac{1}{\upsilon_e} & \frac{\partial \upsilon}{\partial Ku_p}\frac{1}{\upsilon_e} & \frac{\partial \upsilon}{\partial Ks_p}\frac{1}{\upsilon} \\ \frac{\partial B}{\partial K_p}\frac{1}{B_e} & \frac{\partial B}{\partial E_p}\frac{1}{B_e} & \frac{\partial B}{\partial Ku_p}\frac{1}{B_e} & \frac{\partial B}{\partial Ks_p}\frac{1}{B} \\ \frac{\partial \upsilon_u}{\partial K_p}\frac{1}{\upsilon_{u_e}} & \frac{\partial \upsilon_u}{\partial E_p}\frac{1}{\upsilon_{u_e}} & \frac{\partial \upsilon_u}{\partial Ku_p}\frac{1}{\upsilon_{u_e}} & \frac{\partial \upsilon_u}{\partial Ks_p}\frac{1}{\upsilon_u} \\ \frac{\partial E_u}{\partial K_p}\frac{1}{E_{u_e}} & \frac{\partial E_u}{\partial E_p}\frac{1}{E_{u_e}} & \frac{\partial E_u}{\partial Ku_p}\frac{1}{E_{u_e}} & \frac{\partial E_u}{\partial Ks_p}\frac{1}{E_u} \end{bmatrix}$$

The Jacobian can be simplified since many of the terms are zero or one.

$$\nabla \mathbf{M}(\bar{\mathbf{x}}) = \begin{bmatrix} \frac{1}{\mathbf{K}_e} & 0 & 0 & 0 \\ 0 & \frac{1}{\mathbf{E}_e} & 0 & 0 \\ 0 & 0 & \frac{1}{\mathbf{Ku}_e} & 0 \\ 0 & 0 & 0 & \frac{1}{\mathbf{Ks}_e} \\ \frac{\partial \upsilon}{\partial \mathbf{K}_p}\frac{1}{\upsilon_e} & \frac{\partial \upsilon}{\partial \mathbf{E}_p}\frac{1}{\upsilon_e} & 0 & 0 \\ \frac{\partial B}{\partial \mathbf{K}_p}\frac{1}{B_e} & 0 & \frac{\partial B}{\partial \mathbf{Ku}_p}\frac{1}{B_e} & \frac{\partial B}{\partial \mathbf{Ks}_p}\frac{1}{B} \\ \frac{\partial \upsilon_u}{\partial \mathbf{K}_p}\frac{1}{\upsilon_{u_e}} & \frac{\partial \upsilon_u}{\partial \mathbf{E}_p}\frac{1}{\upsilon_{u_e}} & \frac{\partial \upsilon_u}{\partial \mathbf{Ku}_p}\frac{1}{\upsilon_{u_e}} & \frac{\partial \upsilon_u}{\partial \mathbf{Ks}_p}\frac{1}{\upsilon_u} \\ \frac{\partial E_u}{\partial \mathbf{K}_p}\frac{1}{E_{u_e}} & \frac{\partial E_u}{\partial \mathbf{E}_p}\frac{1}{E_{u_e}} & \frac{\partial E_u}{\partial \mathbf{Ku}_p}\frac{1}{E_{u_e}} & \frac{\partial E_u}{\partial \mathbf{Ks}_p}\frac{1}{E_u} \end{bmatrix}$$

The best fit set of parameters is found using the nonlinear inversion technique described above. MATLAB^{tm} was used to do the numerical calculations for the inversion. The MATLAB^{tm} script file named elaine (elastic inversion) is attached as Appendix B. The inversions converged to a change in the residual of 10^{-8} within ten iterations. The differentials in the Jacobian were checked by Mathematica^{tm}. The results of the inversion, the Best Fit Set of moduli are shown in Table 2.

Table 2: Best Fit Poroelastic Moduli at 30 MPa

Sample	K (GPa)	E (GPa)	υ	Ku(GPa)	Eu (GPa)	υu	B	Ks(GPa)
Berea Sandstone Sample T4	10.2	20.4	.167	18.9	22.7	.300	.656	34.2
Berea Sandstone Sample T7	7.0	14.8	.148	15.2	16.9	.314	.743	25.4
Berea Sandstone Sample T8	6.8	14.9	.137	14.2	16.9	.299	.720	24.6
Berea Sandstone Sample T9	8.7	16.4	.186	16.7	18.2	.318	.690	28.4
Average of Berea Sandstone Samples	8.7	17.8	.160	16.8	19.9	.302	.699	27.9
Indiana Limestone Sample InL1	20.5	28.7	.267	31.9	30.4	.341	.504	70.9
Indiana Limestone Sample InL2	21.9	32.6	.252	31.5	34.3	.319	.432	74.1

Comparison to Previous Work

Values for poroelastic moduli for Berea Sandstone are given by Rice and Cleary (1976). A value of Skempton's coefficient is also given by Berge, Wang, and Bonner (1993). These values are below with the average of the best fit sets for Berea Sandstone found in this experiment for comparison.

Table 3:
Comparison of Best Fit Berea Sandstone Values to Previous Work

Source	K(GPa)	E (GPa)	υ	Ku(GPa)	Eu(GPa)	υu	B	Ks(GPa)
Average of Berea Best Fit Sets	8.7	17.8	0.16	16.8	19.9	0.30	0.70	27.9
Rice and Cleary Set	8.0[1]	14.4[1]	0.20	16.0[1]	16.0[1]	0.33[1]	0.62[1]	36.0[2]
Berge, Wang and Bonner, 1993	--	--	--	--	--	--	0.67 -0.72	--

1. These values were calculated from an experimentally measured Shear Modulus and Poisson's Ratio and an assumed value for the bulk Grain Modulus.
2. This is the value for the bulk modulus of the solid phase for pure quartz.

The values calculated using the experimental data and assumptions from Rice and Cleary (1976) match well with the results given here for the Best Fit Set. The value of the best fit unjacketed

bulk modulus (Ks) is smaller than the unjacketed bulk modulus (Ks) given in Rice and Cleary (1976). The Rice and Cleary (1976) value of Ks does not include the effect of the high clay content found in the Berea Sandstone on Ks. The smaller best fit result for Ks is likely due to the clay. The value of Skempton's coefficient (B) given by Berge, Wang, and Bonner (1993), does not vary significantly from the Best Fit result given by this experiment.

Values for elastic moduli for Indiana Limestone are found in Huang (1989) and Michalopoulos and Triandifilidis (1976). These values are shown below with the average of the best fit values for Indiana Limestone found in this experiment.

Table 4:
Comparison of Best Fit Indiana Limestone Values to Previous Work

Source	K(GPa)	E (GPa)	υ	Ku(GPa)	Eu(GPa)	υu	B	Ks(GPa)
Average of Indiana Limestone Best Fit Sets	21.2	30.7	0.26	31.7	32.4	0.33	0.47	72.5
Huang's Set @ 30 MPa, 1989	26.1	33.7	0.25	33.6[1]	34.6[1]	0.33[1]	0.29[1]	82.1
Handbook Value Michalopoulos and Triandifilidis,1976	--	31.7	0.27	--	--	--	--	--

1. These values were calculated using the four experimental moduli.

The Best Fit values from this experiment match the experimental values from both Huang's thesis and from Michalopoulos and Triandifilidis (1976) within the given experimental error. The value of K is much lower for the average of the Best Fit Set than for Huang's measured K. The Huang's value given in the table is an average of four samples. One of those samples gives a value of K of 21.3 GPa. This is a difference between the two K values of less than 1%. Also the value of

Ks is lower in the Best Fit Set than for Huang's average. Again one of the four samples measured by Huang gives a result of Ks=73.4 GPa. There is not a significant difference between the experimental results.

However there is a significant difference between the calculated value from Huang's data for Skempton's coefficient (B) and the best fit result for B. The value of B was calculated from Huang's data using a relationship found in Rice and Cleary (1976). That relationship is

$$B = \frac{1/K - 1/Ks}{1/K - 1/Ks + \phi(1/K_f - 1/K_\phi)}$$

where $K_\phi = Ks$ is assumed. K_ϕ is the pore bulk modulus and ϕ is the porosity. The difference between the B values is likely due to the greater average K and Ks values of Huang (1989). Also the elastic values measured by Huang are not self consistent. A best fit set of elastic constants might better approximate K and thus the calculated value of B might be closer to the best fit value of B.

Also the above relationship may not be valid for calculating B since the assumption $K_\phi = Ks$ may not hold. The first explanation is more likely.

Testing Goodness of Fit

Comparison of the best fit moduli to the measured moduli tests how well the poroelastic model fits the data. The percent differences are shown in Table 5 below. The Berea Sandstone samples all show similar trends away from the theory. For example the measured bulk modulus is always greater than the best fit bulk modulus. Not only do the percent differences have the same sign but their magnitudes are similar. This means random errors in measurement are not likely responsible for the difference. The Indiana Limestone moduli do not

show consistent trends. One sample may show a larger value for the measured modulus than the best fit modulus while for other moduli both samples may be higher or lower. These differences are more likely caused by random error from the measurements.

Another measure of fit to the theory is the root mean squared error, $(r^t r)^{1/2}/8$. The Berea Sandstone consistently has a greater error than the Indiana Limestone. These two results show that Indiana Limestone will behave according to poroelastic theory more closely than will Berea Sandstone.

Table 5: Percent Difference between Measured and Best Fit Moduli

Sample $100\times$	$\frac{\Delta K}{K_e}$	$\frac{\Delta E}{E_e}$	$\frac{\Delta \upsilon}{\upsilon_e}$	$\frac{\Delta Ku}{Ku_e}$	$\frac{\Delta Eu}{Eu_e}$	$\frac{\Delta \upsilon_u}{\upsilon_{u_e}}$	$\frac{\Delta B}{B_e}$	$\frac{\Delta Ks}{Ks_e}$	RMS Error
Berea Sandstone Sample T4	23.9	26.5	-9.9	-12.5	-22.0	18.7	8.2	3.3	0.062
Berea Sandstone Sample T7	46.3	37.3	-12.4	-1.0	-37.3	-3.0	11.8	4.2	0.091
Berea Sandstone Sample T8	50.3	36.6	-10.3	-15.2	-28.2	19.9	16.8	5.7	0.095
Berea Sandstone Sample T9	38.4	37.3	-12.0	-6.9	-34.8	-8.6	-8.6	7.8	0.087
Indiana Limestone Sample InL1	6.7	10.8	-4.3	-4.3	-10.5	13.6	0.5	0.2	0.030
Indiana Limestone Sample InL2	4.3	-9.6	1.0	-2.7	9.8	-0.5	0.8	0.4	0.018

Two hypotheses explaining Berea Sandstone's deviation from the poroelastic model have been tested. Both hypotheses have been shown to not be responsible for the deviation.

It was first postulated that testing the samples dry during a drained run caused the samples to be stiffer. The clay in the Berea Sandstone might stiffen the samples when dry but would not stiffen them when wet. The drained moduli for Berea Sandstone Samples T4, T7 and T8 were found when the samples were dry. If clay were responsible

for the bias we would expect the measured values of the drained bulk modulus to be greater than the values of the best fit bulk modulus. This is because the best fit set of moduli would take into account the less stiff medium measured during the undrained tests and would lower the values of the drained bulk modulus accordingly.

This can be looked at from another view. It is shown in Appendix A that the drained shear modulus and the undrained shear modulus are equal, $G=G_U$. These values are calculated in Table 6, shown below, using the relationships

$$G=\frac{E}{2(1+\upsilon)} \quad \text{and} \quad G_u=\frac{E_u}{2(1+\upsilon_u)}$$

and experimental values of the drained and undrained Young's modulus and Poisson's ratio. If clay is responsible for stiffening the samples when they are dry, then the G calculated when dry should be greater than G_u calculated when the sample is wet. This is the case for Samples T4, T7 and T8. It appears that clay could cause the bias when looking only at samples T4, T7 and T8.

However, the drained moduli for Berea Sample T9 were tested under wet and drained conditions and Sample T9 shows a trend similar to the other Berea Sandstone samples away from the best fit results. The drained and undrained shear moduli calculated for Sample T9 have very similar to values from Samples T4, T7 and T8. The presence of water during the drained tests did not eliminate or even significantly reduce the bias observed. Since invoking clay as the cause of the bias works so well theoretically and only one sample was tested drained and wet, other samples should be tested drained and wet to better test this hypothesis.

Table 6: Calculated Shear Moduli

Sample	Calculated Drained Shear Modulus	Calculated Undrained Shear Modulus
Berea Sandstone Sample T4	11.9	6.7
Berea Sandstone Sample T7	10.4	4.7
Berea Sandstone Sample T8	10.5	4.8
Berea Sandstone Sample T9	11.2	5.2

The second explanation for the deviation from theory involved sample anisotropy. The drained and undrained bulk modulus tests are performed under hydrostatic confining pressure. Under hydrostatic stress conditions an ideal sample would strain exactly the same amount in the circumferential and axial directions. Ratios of circumferential strain to axial strain under hydrostatic stress were found for the samples. Table 7 below of anisotropy ratios for hydrostatic tests at 30 MPa show there is no strict correlation between the anisotropy and the deviation from theory. Sample T4 has ratios greater than 1 but still behaves in approximately the same manner as Samples T7,T8, and T9.

Table 7: Anisotropy Ratios for Hydrostatic Tests at 30 MPa.

Sample	Anisotropy During Drained Bulk Modulus Test ($\varepsilon\theta\theta/\varepsilon zz$)	Anisotropy During Undrained Bulk Modulus Test ($\varepsilon\theta\theta/\varepsilon zz$)
Berea Sandstone Sample T4	1.07	1.06
Berea Sandstone Sample T7	0.91	0.78
Berea Sandstone Sample T8	1.13	0.81
Berea Sandstone Sample T9	0.81	0.68
Indiana Limestone Sample InL1	0.93	0.86
Indiana Limestone Sample InL2	1.18	1.25

Calculations of Three More Moduli Using the Best Fit Set

The best fit set of moduli can be used to calculate values of other poroelastic moduli. Values of three more moduli were calculated. The three moduli are the vertical compressibility (α), specific storage (Ss) and the barometric efficiency (γ). Two of these moduli, the vertical compressibility and the barometric efficiency, are of special interest to hydrogeologists.

The first two moduli calculated from the best fit set of moduli are the vertical compressibility and the specific storage. The vertical compressibility is defined as

$$\alpha = \frac{1}{V}\left(\frac{\partial V}{\partial \sigma_{33}}\right)\Bigg|_{\varepsilon_{11}=\varepsilon_{22}=0, dp=0}.$$

This can be calculated from the best fit set using K and υ and the relationship $\alpha = 3K\frac{1-\upsilon}{1+\upsilon}$.

The specific storage (Ss) is rigorously defined in Green and Wang (1990), as

$$Ss = g\frac{dm_f}{dp}\Bigg|_{\sigma 33=0, \varepsilon 11=\varepsilon 22=0}.$$

Green and Wang (1990) developed an expression relating the specific storage to other poroelastic moduli. This expression is

$$Ss = \rho_f g\left[\left(\frac{1}{K}-\frac{1}{Ks}\right)\left(1-\frac{4G(1-K/Ks)/3}{K+4G/3}\right)+\phi\left(\frac{1}{K_f}-\frac{1}{Ks}\right)\right].$$

Here ρ_f is the fluid density, g is the acceleration of gravity, G is the shear modulus to be calculated from best fit values of K and E, and ϕ is the porosity of the medium. K_f is the fluid bulk modulus. A simplification of the above expression can be made if the bulk grain modulus (Ks) is assumed to be very large. This implies the grains are

incompressible. The expression for the specific storage reduces to the usual one seen in Domenico and Schwartz (1990). The reduced expression is

$$Ss = \rho_f g\left[\alpha + \phi\frac{1}{K_f}\right].$$

α is the vertical compression discussed above. A table of calculated values for the vertical compressibilities, the full specific storage coefficient, and the reduced specific storage coefficient are given below.

Table 8: Calculated values for α and Ss

Sample	Vertical Compressibility (Pa^{-1})	Specific Storage full expression (m^{-1})	Specific Storage reduced expression (m^{-1})
Average Berea Sandstone	5.28×10^{-11}	7.92×10^{-7}	8.90×10^{-7}
Average Indiana Limestone	2.67×10^{-11}	4.60×10^{-7}	5.09×10^{-7}

Values used for the calculations were ϕ=0.19 for the Berea Sandstone and ϕ=0.13 for the Indiana Limestone and Kf=5×10^9 Pa.

The third modulus calculated is called the barometric efficiency (Van der Kamp and Gale, 1983). The barometric efficiency is defined as

$$\gamma = \left.\frac{\partial p}{\partial \sigma_{11}}\right|_{\varepsilon_{22}=\varepsilon_{33}=0}$$

It can be calculated from undrained Poisson's ration (υ_u) and Skempton's coefficient (B) using the relationship

$$\gamma = \frac{B(1+\upsilon_u)}{3(1-\upsilon_u)}.$$

The value of the barometric efficiency was also experimentally measured for Indiana Limestone Sample InL1 and Berea Sandstone

Sample T9. These values are then compared in the table below to calculated values using the best fit values for B and υ.

Table 9:
Experimental and Calculated Values for the Barometric Efficiency

Sample	experimental γ	best fit B and υ γ
Berea Sandstone Sample T9	0.45	0.44
Indiana Limestone Sample InL1	0.33	0.34

Conclusion

In this experiment eight poroelastic moduli were measured for two rock types, Berea Sandstone and Indiana Limestone. Since only four moduli are needed to completely characterize a fluid-filled porous medium these sets of eight moduli are overdetermined. Inversions of those sets of eight moduli to find Best Fit Sets of moduli were done. Comparisons of the best fit sets to the measured sets could show a bias in the measurements. In the case of Berea Sandstone that bias is present. It is unknown at this time whether that bias is due to the measuring technique or is simply the way Berea Sandstone actually behaves. If only four or fewer moduli were measured then this bias would still exist but would not be apparent. Indiana Limestone showed no bias when comparing the best fit set of moduli to the measured set of moduli.

By both overdetermining the set of poroelastic moduli and then inverting that set, the experimenter has a new tool to check both the applicability of poroelastic theory to the medium in question and the technique of measurement. The goal of finding a better set of poroelastic moduli to represent the medium in question is made easier.

References

Berge, P. A., Wang, H. F., and Bonner, B. P. (1993), *Pore Pressure Buildup Coefficient in Synthetic and Natural Sandstones,* Int. J. Rock Mech. Min. Sci. and Geomech. Abstr. (submitted for publication).

Bethke, C. M., and Corbet, T. F. , *Linear and nonlinear solutions for one-dimensional compaction flow in sedimentary basins,* Water Resour. Res., 24, 461-467, 1988.

Biot, M. A. (1941), *General Theory of Three-dimensional Consolidation,* J. Appl. Physics 12, 155-164

Bredehoeft, J.D., *Response of the ground-water system at Yucca Mountain to an earthquake,* In Groundwater at Yucca Mountain (National Academy Press, Washington, D. C. 1992) pp. 212-222.

Carrigan, C., King, G.P., Barr, G. E., and Bixler, N.E. (1991), *Potential for Water Table Excursions Induced by Seismic Events at Yucca Mountain,* Nevada, Geology 19, 1157-1160.

Detournay, E., and Cheng, A. H.-D., *Fundamentals of Poroelasticy,* Comprehensive Rock Engineering, Volume 2, Chapter 5, J. Hudson ed., Pergeman Press, 1993

Domenico, P. A., and Schwartz, F. W., *Physical and Chemical Hydrogeology*, (John Wiley and Sons, Inc.,1990)

Dropek, R. K., Johnson, J. N., and Walsh, J. B. (1978), *The influence of Pore Pressure on the mechanical properties of Kayenta Sandstone,* J. Geophys. Res., 90, 953-979.

Green, D. H., and Wang, H. F. (1986), *Fluid Pressure Response to Undrained Compression in Saturated Sedimentary Rock*, Geophysics 51, 948-956.

Green, D.H. and Wang, H.F. (1990), *Specific Storage as a Poroelastic Coefficient*, Water Resources Research, Vol. 26, No. 7, 1631-1637.

Haimson, B. C., and Fairhurst, C. (1969), *Hydraulic fracturing in porous-permeable materials*, J. Pet. Technol. 21, 811-817.

Huang, X. (1989), *The Effect of Pore Pressure on Hydraulic Fracturing*, (M. S. thesis, University of Wisconsin-Madison, 1989).

Lama, R. D., and Vutukuri, V. S. , *Handbook on Mechanical Properties of Rocks*, Vol. 2, Trans Tech Publications, 1978.

Menke, W., *Geophysical Data Analysis: Discrete Inverse Theory*, 2nd. ed., (Academic Press, Inc., 1989).

Michalopoulos, A. P., and Triandafilidis, G. E., *Influence of water on hardness, strength and compressibility*, Bull. Assoc. Eng. Geol., Vol. XIII, No. 1, 1976, 1-12.

Nur, A., and Byerlee, J.D. (1971), *An Exact Effective Stress Law for Elastic Deformation of Rocks with Fluids*, Journal of Geophysical Research, Vol. 76, No. 26, 6414-6419.

Rice, J. R., and Cleary, M. P. (1976), *Some Basic Stress-diffusion Solutions for Fluid-saturated Elastic Porous Media with Compressible Constituents*, Rev. Geophys. Space. Phys. 14, 227-241

Segall, P. (1989), *Earthquakes Triggered by Fluid-Extraction*, Geology 17, 942-946.

Van der Kamp, G., and Gale, J. E. (1983), *Theory of Earth Tide and Barometric Effects in Porous Formations with Compressible Grains*, Water Resources Res. 19, 538-544.

Appendix A - Derivations of Relationships Between Moduli

Derivation of $\mathbf{B}=\frac{(1-\frac{K}{Ku})}{(1-\frac{K}{Ks})}$.

The constitutive equations of poroelasticity can be written as

$$2G\varepsilon_{ij}=\sigma_{ij}-\frac{1}{3}\left(1-\frac{2G}{3K}\right)\sigma_{kk}\delta_{ij}+\frac{2G}{3}\left(\frac{1}{K}-\frac{1}{Ks}\right)p\delta_{ij} \text{ and } v_f-v_{f_o}=\left(\frac{1}{K}-\frac{1}{Ks}\right)\left[\frac{\sigma_{kk}}{3}+\frac{1}{B}p\right].$$

These equations are the result of substituting

$$\frac{1}{K}-\frac{1}{Ks}=\frac{1}{H}$$

into the constitutive equations found in Rice and Cleary (1976). The substitution is justified in Nur and Byerlee (1971). The undrained bulk modulus, K_u, is defined as

$$K_u=-V\frac{\partial\sigma_{kk}}{\partial V}\bigg|_{\Delta mf=0,\sigma_{11}=\sigma_{22}=\sigma_{33}}.$$

When the boundary conditions for K_u are applied to the constitutive equations, the result is

$$2G\varepsilon_{ij}=\frac{2G}{9K}\sigma_{kk}+\frac{2G}{3}\left(\frac{1}{K}-\frac{1}{Ks}\right)p\delta_{ij} \quad \text{and} \quad p=-\frac{B\sigma_{kk}}{3}.$$

Substituting for p into the first equation gives

$$\varepsilon_{kk}=\frac{1}{K}\frac{\sigma_{kk}}{3}-\frac{B}{3}\left(\frac{1}{K}-\frac{1}{Ks}\right)\sigma_{kk}.$$

This equation is rearranged so that

$$\frac{1}{K}-B\left(\frac{1}{K}-\frac{1}{Ks}\right)=\frac{\varepsilon_{kk}}{\sigma_{kk}/3}.$$

Since $\frac{\varepsilon_{kk}}{\sigma_{kk}/3}=\frac{\Delta V}{V}\frac{1}{\sigma_{kk}}$ is the definition of $1/K_u$ then $\frac{1}{Ku}=\frac{1}{K}-B\left(\frac{1}{K}-\frac{1}{Ks}\right)$.

This can be arranged so that

$$\mathbf{B}=\frac{(1-\frac{K}{Ku})}{(1-\frac{K}{Ks})}.$$

Derivation of $\upsilon = \frac{1}{2} - \frac{E}{6K}$.

This is the usual elastic relationship between υ, E and K. Since $\Delta p = 0$, the pore pressure term is zero so the first constitutive equation of poroelasticity is identical to the constitutive equation for elasticity. The relationships derived for elasticity hold for drained poroelastic moduli.

Derivation of $\upsilon_u = \frac{3\upsilon + B(1-2\upsilon)(1-K/K_s)}{3 - B(1-2\upsilon)(1-K/K_s)}$.

The definition of the undrained Poisson's ratio is

$$\upsilon_u = -\left.\frac{\varepsilon_{22}}{\varepsilon_{11}}\right|_{\Delta mf=0,\,\sigma_{22}=\sigma_{33}=0}.$$

The starting constitutive equations for poroelasticity again are

$$2G\varepsilon_{ij} = \sigma_{ij} - \frac{1}{3}\left(1 - \frac{2G}{3K}\right)\sigma_{kk}\delta_{ij} + \frac{2G}{3}\left(\frac{1}{K} - \frac{1}{Ks}\right)p\delta_{ij} \text{ and } v_f - v_{f0} = \left(\frac{1}{K} - \frac{1}{Ks}\right)\left[\frac{\sigma_{kk}}{3} + \frac{1}{B}p\right].$$

When the stress and pore fluid boundary conditions are applied to the constitutive equations the result is

$$2G\varepsilon_{11} = \sigma_{11} - \frac{\sigma_{11}}{3} + \frac{2G}{9K}\sigma_{11} + \frac{2G}{3}\left(\frac{1}{K} - \frac{1}{Ks}\right)p \text{ and } 2G\varepsilon_{22} = -\frac{\sigma_{11}}{3} + \frac{2G}{9K}\sigma_{11} + \frac{2G}{3}\left(\frac{1}{K} - \frac{1}{Ks}\right)p$$

from the first equation for the strains, ε_{11} and ε_{22}, and

$$p = -\frac{B\sigma_{kk}}{3}$$

from the second equation for undrained pore fluid condition. The definition of the Undrained Poisson's Ratio is applied and p is replaced.

$$\frac{2G\varepsilon_{22} = -\frac{\sigma_{11}}{3} + \frac{2G}{9K}\sigma_{11} - \frac{2G}{3}\left(\frac{1}{K} - \frac{1}{Ks}\right)\frac{B}{3}\sigma_{11}}{2G\varepsilon_{11} = \sigma_{11} - \frac{\sigma_{11}}{3} + \frac{2G}{9K}\sigma_{11} - \frac{2G}{3}\left(\frac{1}{K} - \frac{1}{Ks}\right)\frac{B}{3}\sigma_{11}}$$

Some simplification of the ratio on the previous page is done by canceling the $2G$'s on the left hand side and a factor of $\sigma_{11}/3$ on the right hand side. The result after some algebra, remembering the negative sign in the definition of Poisson's ratio, is

$$\upsilon_u = \frac{3\upsilon + B(1-2\upsilon)(1-K/K_s)}{3 - B(1-2\upsilon)(1-K/K_s)}.$$

Derivation of $G = Gu$

Since the pore fluid can exert no shear stress, the result, $G = Gu$, might be intuitive. The constitutive equations of poroelasticity are

$$2G\varepsilon_{ij} = \sigma_{ij} - \frac{1}{3}\left(1 - \frac{2G}{3K}\right)\sigma_{kk}\delta_{ij} + \frac{2G}{3}\left(\frac{1}{K} - \frac{1}{Ks}\right)p\delta_{ij} \text{ and } v_f - v_{f0} = \left(\frac{1}{K} - \frac{1}{Ks}\right)\left[\frac{\sigma_{kk}}{3} + \frac{1}{B}p\right].$$

When the boundary conditions for the drained shear modulus, $\Delta p = 0$ and $i \neq j$, are applied to the first equation, the definition of the drained shear modulus is returned as expected,

$$2G = \frac{\sigma_{ij}}{\varepsilon_{ij}}.$$

When the pore fluid boundary condition is changed to undrained, $\Delta m_f = 0$, the result is the same,

$$2G = \frac{\sigma_{ij}}{\varepsilon_{ij}}.$$

This is because $i \neq j$ causes all terms but the shear terms to be zero. The pore pressure and fluid volume terms are never part of the shear terms.

Derivation of $Eu = 3Ku(1-2\upsilon_u)$

This derivation begins by first using the elastic relationship between the drained shear modulus, the drained bulk modulus, and the drained Poisson's ratio,

$$G = \frac{3K}{2}\frac{(1-2\upsilon)}{(1+\upsilon)}.$$

The equation above can be rewritten as

$$G = \frac{3K}{2(1-\alpha B)}\frac{3}{3}\frac{[(1-2\upsilon)-\alpha B(1-2\upsilon)]}{(1+\upsilon)}$$

by multiplying top and bottom by

$$\frac{3}{3}\frac{(1-\alpha B)}{(1-\alpha B)}.$$

That equation can manipulated into the form

$$G = \frac{3K}{2(1-\alpha B)}\left[\frac{1-\dfrac{6\upsilon+2\alpha B(1-2\upsilon)}{3-\alpha B(1-2\upsilon)}}{1+\dfrac{3\upsilon+\alpha B(1-2\upsilon)}{3-\alpha B(1-2\upsilon)}}\right]$$

where

$$\alpha = 1-\frac{K}{Ks}.$$

Since

$$Ku = \frac{K}{1-\alpha B} \qquad \text{and} \qquad \upsilon_u = \frac{3\upsilon+\alpha B(1-2\upsilon)}{3-\alpha B(1-2\upsilon)},$$

Ku and υ_u can be substituted into the relationship above. The result is

$$G = \frac{3Ku}{2}\left[\frac{1-2\upsilon_u}{1+\upsilon_u}\right].$$

The next step is to show the relationship between the undrained Young's modulus, the shear modulus, and the undrained bulk modulus.

The definition of the undrained Young's modulus is

$$E_U = \left.\frac{\sigma_{11}}{\varepsilon_{11}}\right|_{dm_f=0,\,\sigma_{22}=\sigma_{33}=0}.$$

When the boundary conditions are applied to the constitutive equations the result is

$$2G\varepsilon_{11} = \sigma_{11} - \frac{1}{3}\left(1 - \frac{2G}{3K}\right)\sigma_{11} + \frac{2G}{3K}\alpha p \quad \text{and} \quad p = -\frac{B}{3}\sigma_{kk}$$

where

$$\alpha = 1 - \frac{K}{Ks}.$$

Rearranging terms gives

$$\frac{\sigma_{11}}{\varepsilon_{11}} = \frac{9GKu}{3Ku + G}$$

so

$$Eu = \frac{9GKu}{3Ku + G}.$$

The last step is to now eliminate the shear modulus from the above expression.

$$G = \frac{3Ku}{2}\left[\frac{1 - 2\upsilon_u}{1 + \upsilon_u}\right]$$

has been shown and can be substituted. After some algebra the result is the desired one,

$$Eu = 3Ku(1 - 2\upsilon_u).$$

Appendix B

The MATLAB^{tm} script file elaine.

```
% elain (elastic inverse) will invert eight elastic constants
% Nu(Poisson's Ratio), K(bulk Modulus), E(Young's Modulus) all under
% drained and undrained conditions, B(Skempton's Coefficient)
% and Ks (bulk Grain Modulus). These parameters are all
% given as data. The inversion will output the four best fit constants,
% here K, E, Ku, Ks.
% Initially b(1)=K, b(2)=E, b(3)=Ku, and b(4)=Ks. The other parameters
% are then calculated from these four. So b(5-8) doesn't necessarily
equal
% the other  experimental constants.
% This inversion doesn't assume that Kphi=Ks.
% This inversion also doesn't need Kf or porosity.

% Setting up house by giving parameters initial values and setting
% control variables to big values.

K=b(1);
E=b(2);
Ku=b(3);
Ks=b(4);
V=1/2-E/(6*K)
B=(1/K-1/Ku)/(1/K-1/Ks)
Vu=(3*V+B*(1-2*V)*(1-K/Ks))/(3-B*(1-2*V)*(1-K/Ks))
Eu=3*Ku*(1-2*Vu)

Avenew=1;
change=1;

% Loops until residual average does not change.

while  change>(.00000001)

% calcres
%
% This routine will calculate the residuals between the data
% and the calculated elastic parameters.
% The residual is normalized here.
```

```
r(1)=1-K/b(1);
r(2)=1-E/b(2);
r(3)=1-Ku/b(3);
r(4)=1-Ks/b(4);
r(5)=1-V/b(5);
r(6)=1-B/b(6);
r(7)=1-Vu/b(7);
r(8)=1-Eu/b(8);

Aveold=Avenew;
 aver=sqrt(r'*r)/8
Avenew=aver;
  change=abs((Aveold-Avenew)/Avenew);

% CalcA
%
% This routine will calculate the A matrix(the Jacobian)
% the Jacobian is normalized.
  dVdK= E/(6*K^2);

  dVdE= -1/(6*K);

   dBdK= 1/(K^2)*(-1/(1/K-1/Ks) + (1/K-1/Ku)/(1/K-1/Ks)^2);

   dBdKs=-(1/K-1/Ku)/((Ks^2)*(1/K-1/Ks)^2);

   dBdKu=1/(Ku^2)*(1/(1/K-1/Ks));

  den=3-B*(1-2*V)*(1-K/Ks);
  num=3*V+B*(1-2*V)*(1-K/Ks);

  C1=3*dVdK+dBdK*(1-2*V)*(1-K/Ks)+B*(-2*dVdK)*(1-K/Ks)+B*(1-
2*V)*(-1/Ks);
  C4=dBdK*(1-2*V)*(1-K/Ks)+B*(-2*dVdK)*(1-K/Ks)+B*(1-2*V)*(-1/Ks);
  dVudK=C1/den + num/den^2*C4;

  C1=3*dVdE+B*(-2*dVdE)*(1-K/Ks);
  C4=B*(2*dVdE)*(1-K/Ks);
   dVudE=C1/den-num/den^2*C4;

  C1=dBdKs*(1-2*V)*(1-K/Ks)+B*(1-2*V)*(K/Ks^2);
  dVudKs=C1/den + num/den^2*C1;
```

```
C1=dBdKu*(1-2*V)*(1-K/Ks);
dVudKu=C1/den + num/den^2*C1;

dEudK=3*Ku*(-2*dVudK);

dEudE=3*Ku*(-2*dVudE);

dEudKu=3*(1-2*Vu) + 3*Ku*(-2*dVudKu);

dEudKs=3*Ku*(-2*dVudKs);

delM=[];
delM=[1/b(1)      0          0          0
      0         1/b(2)      0          0
      0         0          1/b(3)      0
      0         0          0          1/b(4)
      dVdK/b(5)   dVdE/b(5)    0          0
      dBdK/b(6)   0          dBdKu/b(6)   dBdKs/b(6)
      dVudK/b(7)  dVudE/b(7)   dVudKu/b(7)  dVudKs/b(7)
      dEudK/b(8)  dEudE/b(8)   dEudKu/b(8)  dEudKs/b(8) ];

A=delM;

% calcdelx
%
% This routine calculates the change in parameters necessary
% to meet the goal of finding the parameters which will let
% Model(X+delx)=data

Q=inv(A'*A);
delx=Q*A'*r;

% calcpar
%
% This routine calculates new values for the parameters which
% can then be used to iterate the model again.

K=K+delx(1);
E=E+delx(2);
Ku=Ku+delx(3);
Ks=Ks+delx(4);
```

```
    V=1/2-E/(6*K);
     B=(1/K-1/Ku)/(1/K-1/Ks);
     Vu=(3*V+B*(1-2*V)*(1-K/Ks))/(3-B*(1-2*V)*(1-K/Ks));
    Eu=3*Ku*(1-2*Vu);

end         % Ends the while loop.
    r(1)=1-K/b(1);
    r(2)=1-E/b(2);
    r(3)=1-Ku/b(3);
    r(4)=1-Ks/b(4);
    r(5)=1-V/b(5);
    r(6)=1-B/b(6);
    r(7)=1-Vu/b(7);
    r(8)=1-Eu/b(8);
parameters=[K
            E
            Ku
            Ks
            V
            B
             Vu
            Eu];
results=[b,parameters,r*100]
Kphi=1/(vo*(1/Kf-1/Ks) + 1/K - (1/K-1/Ks)/B)
aver
```

Figure 1

Sample Assembly

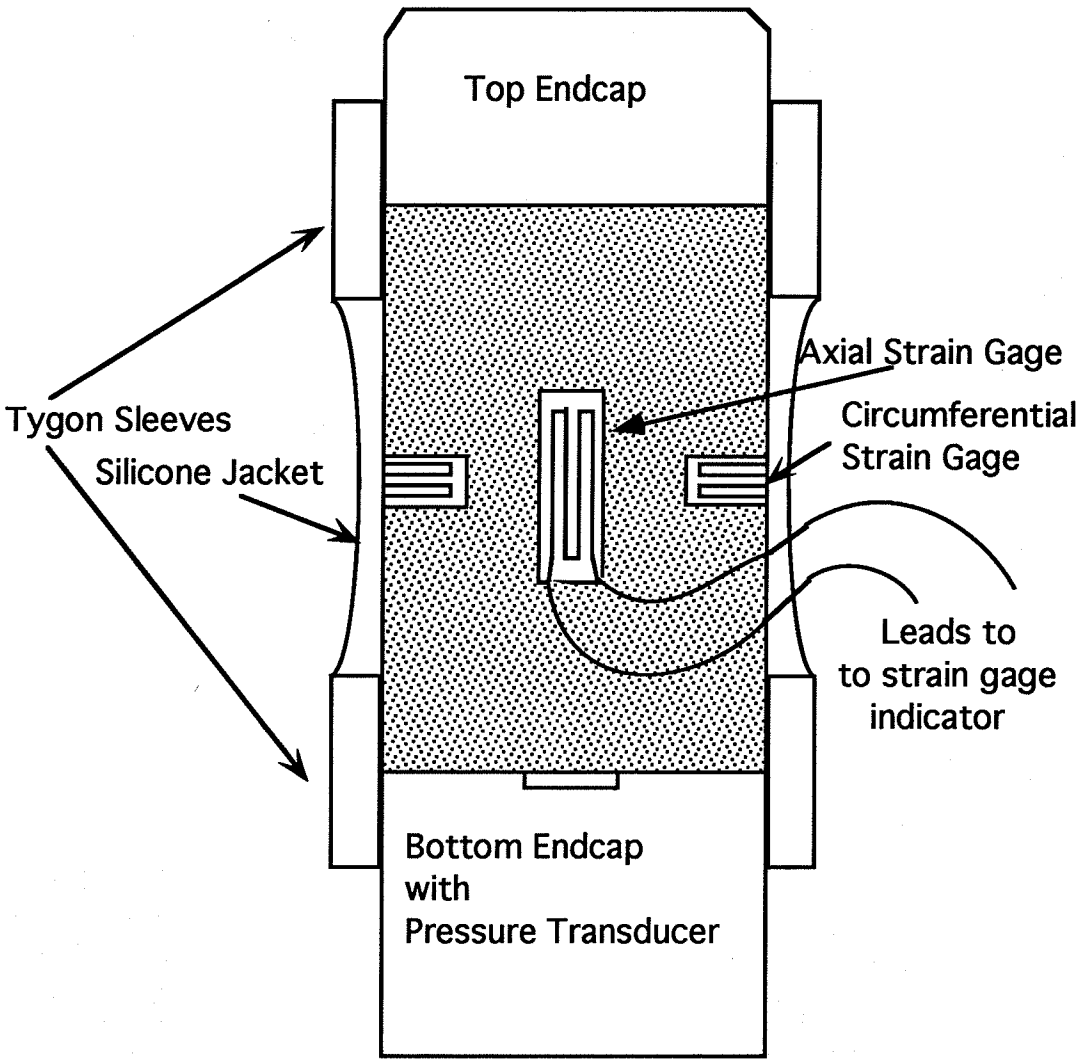

Figure 2 Graphs of Data for Berea Sandstone Sample T4

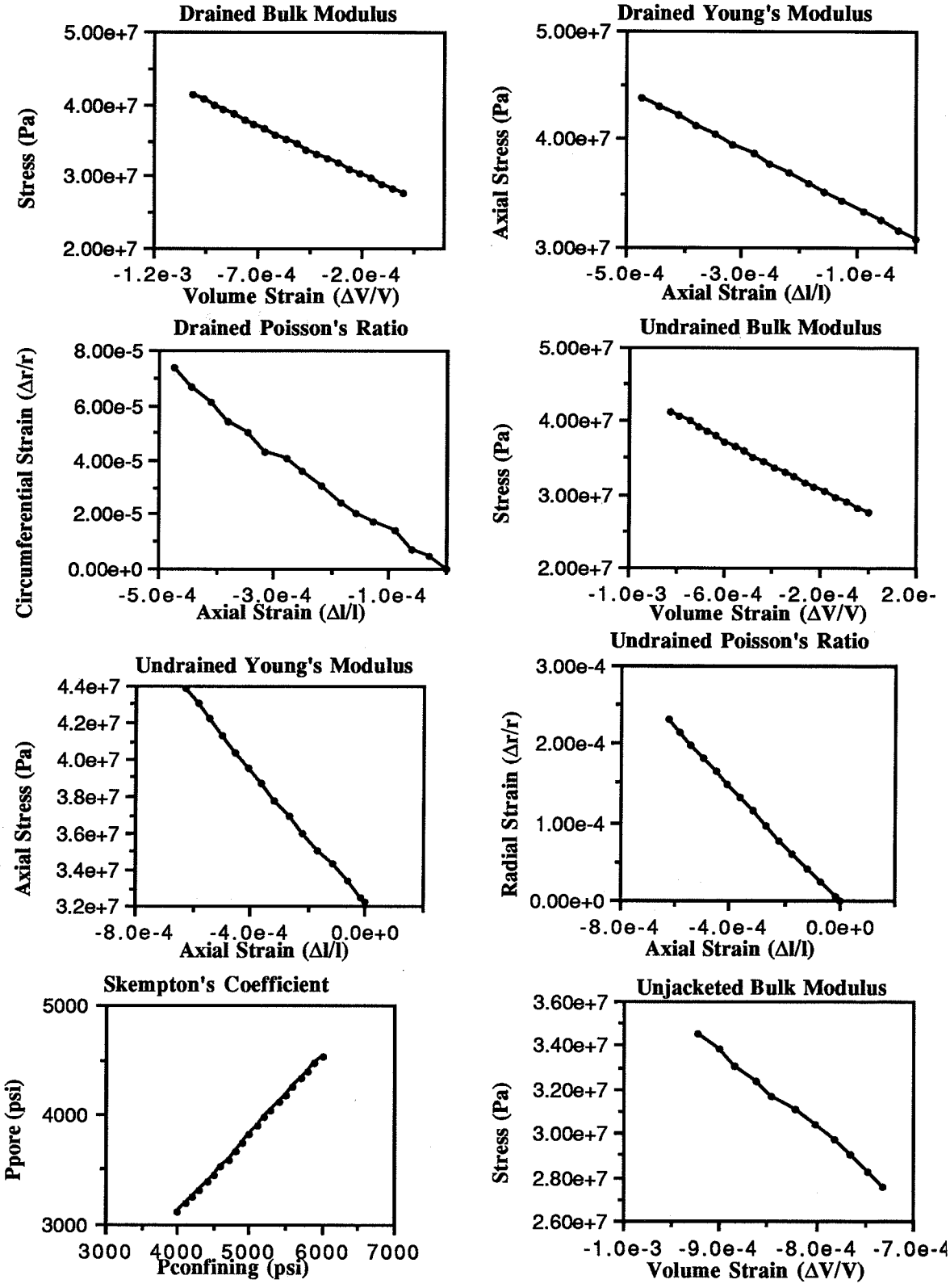

Figure 3 Graphs of Data for Indiana Limestone Sample InL1

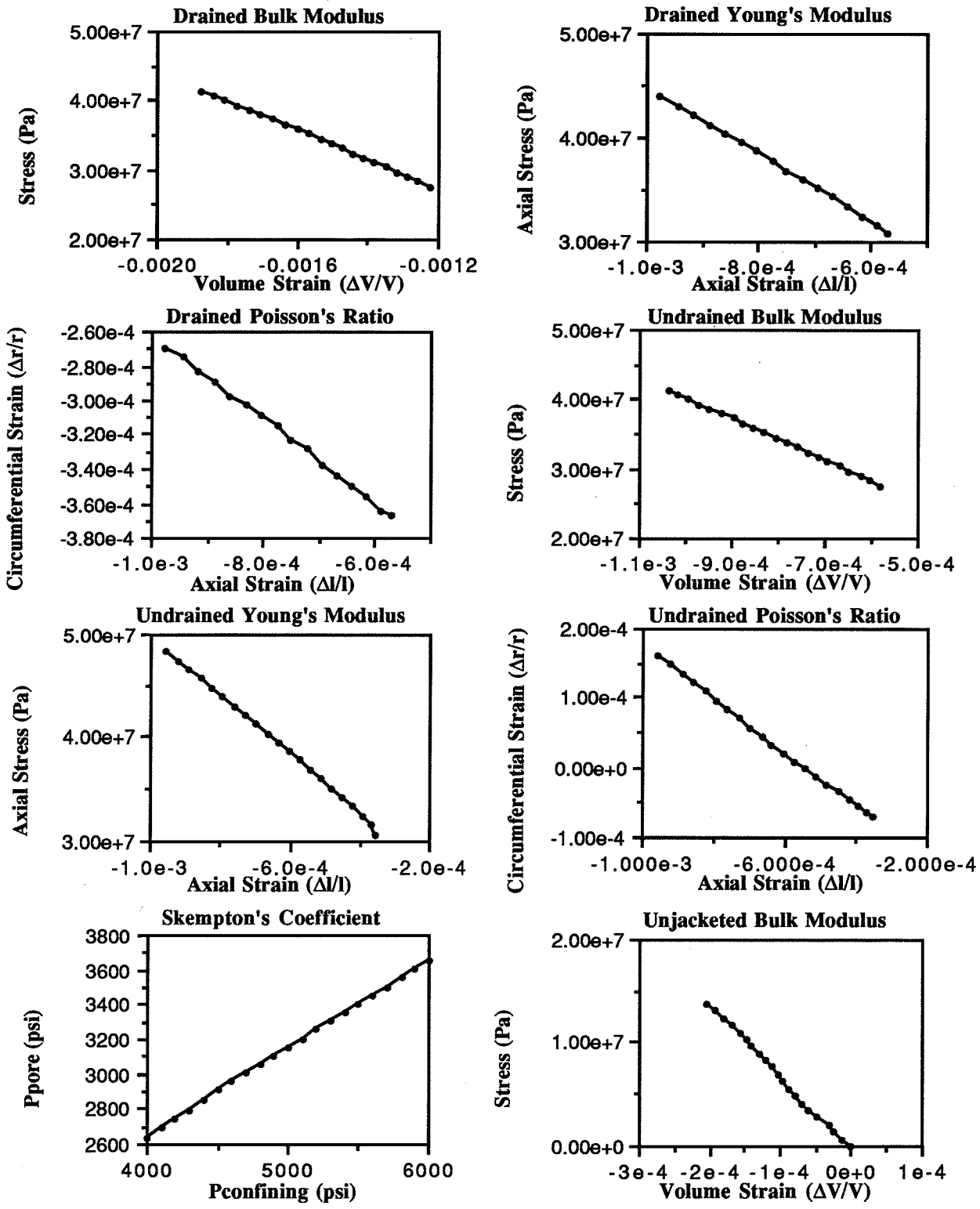

Approved by Herbert F. Wang

Title Professor

Date 5/19/94